Supplemental Methods and Data

The NOD/RIPK2 signaling pathway contributes to osteoarthritis susceptibility

By

Michael J. Jurynec[1][*], Catherine M. Gavile[1], Matthew Honeggar[1], Ying Ma[1], Shivakumar R. Veerabhadraiah[1], Kendra A. Novak[1], Kazuyuki Hoshijima[2], Nikolas H. Kazmers[1], and David J. Grunwald[2]

[1]Department of Orthopaedics, University of Utah, Salt Lake City, UT, USA 84108

[2]Department of Human Genetics, University of Utah, Salt Lake City, UT, USA, 84112

*Corresponding author: Michael J. Jurynec

Contact information: email: mjurynec@genetics.utah.edu; Phone: 801-581-4424; Address: Department of Orthopaedics, University of Utah, 15 N 2030 E, Bldg 533, Salt Lake City, UT, USA 84112

Running head: A human *RIPK2* OA allele increases susceptibility to OA in mice

METHODS

Diagnostic and procedure codes used to identify individuals with osteoarthritis of the 1st MTP joint, distal and proximal interphalangeal joints, and glenohumeral joint

The following diagnostic codes (ICD-9 and ICD-10) and procedure codes (CPT - Current Procedural Terminology) were used to identify affected individuals.

1st MTP joint OA (synonymous with hallux rigidus):

CPT: 28289 (hallux rigidus correction with cheilectomy, debridement and capsular release 1st metatarsophalangeal joint) and 28750 (arthrodesis, great toe).

ICD-9: 735.2 (hallux rigidus).

ICD-10: not used.

Distal and proximal interphalangeal joint OA:

CPT: 26862, 26863, 26860, 26861 (arthrodesis, interphalangeal joint, with or without internal fixation) and 26535, 26536 (arthroplasty, interphalangeal joint).

ICD-9: 715.14 (osteoarthritis, localized, primary, hand).

ICD-10: M19.04x (primary osteoarthritis, hand).

Glenohumeral OA:

CPT: 23472 (arthroplasty, glenohumeral joint).

ICD-9: 715.11 (osteoarthritis, localized, primary, shoulder region).

ICD-10: M19.011 (primary osteoarthritis, right shoulder), M19.012 (primary osteoarthritis, left shoulder), M19.019 (primary osteoarthritis, unspecified shoulder), Z96.611 (presence of right artificial shoulder joint), Z96.612 (presence of left artificial shoulder joint), or M19.0x (primary osteoarthritis, shoulder).

Individuals diagnosed with any of the following codes were excluded:

ICD-9: 714.0 (rheumatoid arthritis), 714.2 and 714.3 (rheumatoid arthritis and other inflammatory polyarthropathies).

ICD-10: M05.xxx (rheumatoid polyneuropathy with rheumatoid arthritis), M06.xx (other rheumatoid arthritis), or M08.xxx (juvenile arthritis).

Individuals were asked if they were diagnosed with psoriatic arthritis, gout, or had a traumatic injury to the affected joint. If they answered yes, they were excluded from the study.

Whole exome sequencing and analysis

Whole exome sequencing (WES) and analysis was performed using genomic DNA isolated from whole blood or saliva as previously described[1]. Libraries were prepared using the Agilent SureSelect XT Human All Exon + UTR (v8) kit followed by Illumina NovaSeq 6000 150 cycle paired end sequencing. We followed best practices established by the Broad Institute GATK for variant discovery (https://gatk.broadinstitute.org/hc/en-us). Analysis of variants was performed with ANNOVAR (http://annovar.openbioinformatics.org/en/latest/)[2] and pVAAST

(http://www.hufflab.org/software/pvaast/)[3] in concert with PHEVOR2 (http://weatherby.genetics.utah.edu/phevor2/index.html)[4]. pVAAST is a probabilistic search tool that classifies variants with respect to the likely effect they have on gene function. It incorporates information including position of a variant within a gene, cross-species phylogenetic conservation, biological function, and pedigree structure. PHEVOR2 works in concert with the output of pVAAST to integrate phenotype, gene function, and disease information for improved power to identify disease-causing alleles. The combination of PVAAST and PHEVOR provides a LOD score, p-value, and overall Score (combination of a composite likelihood ratio test (CLRT) and LOD score to compute a gene-level p-values).

Generation of the *Ripk2[104Asp]* allele

CRISPR/Cas9-stimulated Homology Directed Repair (HDR) was used to edit[5, 6] the WT *Ripk2* (p.104Asn) gene of C57BL/6J mice to generate an isogenic line that expressed the variant Ripk2[104Asp] protein from the native locus. The pair of alleles is analogous to the human WT *RIPK2[104Asn]* and disease-associated *RIPK2[104Asp]* alleles[1]. *Ripk2[Asp104]* mice were generated by the University of Utah Transgenic and Gene Targeting Mouse Core. Briefly, fertilized C57BL/6J eggs were injected at the one or two cell stage with Cas9 ribonucleoprotein complex targeting a site in exon 2 of *Ripk2* within 10 base pairs of the Asn codon, and a DNA oligonucleotide to direct the single amino acid coding change[5, 6]. Injected eggs were transplanted into pseudopregnant females and 53 founder pups were screened for the presence of the edited allele using the PCR method described below. Of the 53 pups genotyped, 4 mice (7.5%) were positive for the

Ripk2^Asp104 allele. Positive PCR products were cloned and analyzed by Sanger sequencing. One founder was homozygous for the *Ripk2^Asp104* allele (1.9%) and three others (5.6%) had small additional mutations near the edited site. The homozygous founder was outcrossed to WT C57BL/6J mice and segregation of the *Ripk2^Asp104* allele was determined by PCR, positive alleles were sequenced, and the *Ripk2^Asp104* (*Ripk2^tm1Mjury*) line was established. The template for homology-directed repair (synthesized by Integrated DNA Technologies) was a 200nt single-stranded oligodeoxynucleotide (ssODN) with ~100bp homology arms on each side of the target site and containing several synonymous substitutions to prevent the Cas9 ribonucleoprotein complex from cutting the locus once it had been modified. An EcoRI restriction endonuclease site was also introduced to allow easy identification of the edited allele. The guide RNA sequence is GTTACTGAATACATGCCAAA(TGG), with the PAM site in parentheses. Genotyping primers are as follows – *Ripk2* gF1 5'-ATTTGCAATGAGCCTGAATTC-3' and *Ripk2* gR1 5'-CTAAAGAGCCATTGGGCATATAC-3'.

MDP and WEHI-345 treatment

MDP was reconstituted in endotoxin-free water, as per manufacturer's instructions (Invivogen). Stock solution was diluted into serum-free media, and cells were treated with a concentration of 10 µg/mL of MDP for 6 hours. WEHI-345 was reconstituted in DMSO as per manufacturer's instructions (MedChemExpress). The working solution was prepared by diluting the stock in 1x PBS, and cells were treated at a final concentration of 1µM for 6 hours. As a control for MDP and WEHI-345 treatment, cells

were treated with an equal volume of endotoxin-free water or 1μM DMSO for 6 hours, respectively.

Destabilization of the medial meniscus surgery and anterior cruciate ligament rupture

DMM surgery, OARSI scoring of OA severity, and scoring of synovitis severity was performed as previously described[7, 8]. Sham surgeries consisted of opening the joint capsule and exposing, but not transecting, the medial meniscotibial ligament. Non-invasive ACL rupture was induced by a single overload cycle of tibial compression as previously described[9]. Sixteen-week old male mice were used in all DMM and ACL rupture experiments.

Histology and Immunohistochemistry

Animals were euthanized and knees were dissected and fixed in 10% neutral buffered formalin at 4°C for 48 hours, processed through an ethanol series, demineralized using FormiCal, equilibrated in xylenes, and embedded in paraffin. 5-6 μm thick tissue sections were cut and mounted onto slides. Tissue sections were deparaffinized and rehydrated as follows: Xylene 3X 5 minutes, 95% EtOH 2X 3 minutes, 70% EtOH 2X 3 minutes, ddH$_2$O 1X 2 minutes, and 1X PBS for 5 minutes. For histological analysis, slides were stained with Toluidine blue. For immunohistochemistry, antigen retrieval was according to the antibody manufacturer's protocol. Primary antibodies used were Mmp13 (Abcam, ab51072), Col2 (Fitzgerald – 10R-C135B), Ripk2 (Abnova –

H00008767-M02), pNF-κB (Thermofisher, 44-711G), CD206 (Abcam, ab64693), and

iNos (Abcam, ab3523). Tissue sections were incubated with primary antibody at 4°C, for

18-24 hours in a humidified chamber, rinsed 3X with PBS, and then blocked with 2.5%

horse serum (Vector Laboratories, MP-7401) for 20 minutes at 25°C. Block solution was

replaced with ImmPress-HRP Horse anti-rabbit/mouse secondary antibody (Vector

Laboratories, MP-7401/ MP-7402-15) and incubated for 30 minutes at room

temperature followed by 2X 5 minute rinses with PBS. Slides were stained with DAB

(Vector Laboratories, SK-4100) for 10-20 minutes, rinsed for 5 minutes with PBS, dried,

and mounted.

Quantification of Immunohistochemistry

The total number of chondrocytes that expressed Mmp13, Col2, Ripk2, pNF-κB,

CD206, and iNos in the medial knee joint (both tibial and femoral condyles) of WT

sham, $Ripk2^{Asp104}$ sham, WT DMM, and $Ripk2^{Asp104}$ DMM mice (all 8 weeks post-

surgery) were counted after immunohistochemical staining. Three independent animals

were analyzed for each experimental condition.

Cytokine measurements

Blood from puncture of the submandibular vein was collected into microfuge tubes and

incubated at 4°C for a minimum of 2 hours. Serum was isolated by centrifuging whole

blood at 1500g for 10 minutes. Cytokine concentrations were determined using the

LEGENDplex Inflammation Panel (BioLegend) according to the manufacturer's protocol.

Primary cell cultures

Primary chondrocytes were cultured as previously described[10]. Briefly, mice were euthanized at postnatal day 21-28. The femur was dislocated from the acetabulum, and the articular cartilage cap was collected from the femoral head using blunt-ended forceps. Cartilage pieces were collected into 1X PBS in a 50 mL conical vial on ice, washed 3 times in 1X PBS, resuspended in collagenase D solution (5 mg/mL in DMEM), and incubated in tissue culture plates overnight. The next day, the suspensions were further dissociated by pipetting, filtered through a 70uM filter, and washed once in complete media. Cells were cultured at a density of 200,000 per mL in 24 well plates for 5-7 days, until adhered to the plate and approximately 80% confluent. Media was changed every 3 days. Bone marrow derived macrophages (BMM) were cultured as previously described[11].

RNA isolation

Total RNA from primary chondrocytes or BMM was isolated using Direct-zol RNA Miniprep Kit (Zymo Research).

Nanostring gene expression analysis

Primary chondrocyte or BMM RNA was used for targeted gene expression analysis using the nCounter Fibrosis Panel (Nanostring), which allows quantification of 770 genes, including many genes that have been associated with the OA phenotype.

Samples were processed and analyzed using the Nanostring nCounter platform by the Molecular Diagnostics Core at the University of Utah. Three biological replicates were used for each condition. Data was analyzed by ROSALIND (https://rosalind.bio/), with a HyperScale architecture developed by ROSALIND, Inc. (San Diego, CA). Read Distribution percentages, violin plots, identity heatmaps, and sample MDS plots were generated as part of the QC step. Normalization, fold changes and p-values were calculated using criteria provided by Nanostring. ROSALIND follows the nCounter Advanced Analysis protocol of dividing counts within a lane by the geometric mean of the normalizer probes from the same lane. Housekeeping probes to be used for normalization are selected based on the geNorm algorithm as implemented in the NormqPCR R library[12]. Fold changes and pValues are calculated using the fast method as described in the nCounter Advanced Analysis 2.0 User Manual. P-value adjustment is performed using the Benjamini-Hochberg method of estimating false discovery rates (FDR).

RNA-sequencing and gene expression analysis

ACL rupture was performed on 16-week-old male mice. Whole knee joints were dissected 10 days post-rupture in RNAlater (ThermoFisher) and stored at -80°C. Mice were euthanized and knee joints were exposed by removing the skin and the majority of muscle surrounding the joint with minimal disruption of the ligaments, tendons, synovium, and infrapatellar fat pad. The femur and tibia were cut approximately 0.5 -1 cm distal from the articular surface. Joints were transferred to new RNAlater solution, rinsed, cut into small fragments, transferred to a tube containing Trizol and 2.8mm

stainless steel beads, and homogenized using the BeadBug microtube homogenizer.

Total RNA was isolated as described above. Total RNA from 4 WT and 4 *Ripk2[104Asp]*

knee joints was used for RNA-sequencing (RNA-seq). RNA-seq, quality control, and

alignment was performed by Novogene. Aligned reads were counted using HTSeq

v0.11.3[13], and the counts were then analyzed for differential gene expression using

median-ratio-normalization[14] with Deseq2 v1.30.0[15]. Fold-changes were calculated by

comparing read counts in *Ripk2[104Asp]* knee joints relative to WT knee joints. Genes with

an adjusted P-value < 0.05 were considered differentially expressed.

Quantitative PCR (qPCR)

DMM surgery was performed unilaterally on 16-week-old male mice. Whole knee joints

were dissected from uninjured (control) or operated (DMM) knees for RNA isolation 10

days post-surgery as described above. 1µg total RNA was reverse transcribed into

cDNA, and quantitative assessment of *Nod1, Nod2*, *Ripk2,* and *β-actin* sequences was

performed as described previously[1]. The copy number of *Nod1*, *Nod2*, *Ripk2* was

normalized to 1,000 copies of β-actin as previously described[16]. Primers used are as

follows: *β-actin* F 5'- GTAACAATGCCATGTTCAAT-3', *β-actin* R 5'-

CTCCATCGTGGGCCGCTCTAG, *Nod1* F 5'- CCTGAAGCAGAACACCACACTG-3',

Nod1 R 5'-CTTGGCTGTGATGCGATTCTGG-3', *Nod2* F 5'-

CCTAGCACTGATGCTGGAGAAG-3', *Nod2* R 5'- CGGTAGGTGATGCCATTGTTGG-

3'*Ripk2* F 5'-TCGTGTGGATCCTCTCTGCTCT-3', *Ripk2* R 5'-

TTCCAGGACAGTGGTGTGCCTT-3'.

**Supplemental Table 1.** Family and Phenotype Details

Family	OA Phenotypes and Individuals Analyzed
FIJ744*	Finger Interphalangeal Joint OA - 3 affected, 1 unaffected. Proband (F), husband (unaffected), sister, and son. All affected individuals were diagnosed with bilateral DIP OA.
UUHR2	1st MTP Joint OA - 1 affected (F), 2 unaffected (M and F). Both proband and father were diagnosed with bilateral 1st MTP joint OA.
FIJ7	Finger Interphalangeal Joint OA -2 affected (F), 1 unaffected (F). Proband and 2 daughters (1 affected and 1 unaffected). All affected individuals were diagnosed with bilateral IP joint OA.
FIJ9	Finger Interphalangeal Joint OA - 3 affected, 1 unaffected. Proband (F), mother, and brother affected. Father unaffected.
MTP25	1st MTP Joint OA - 3 affected, 2 unaffected. Proband (F), daughter, and sister affected. 2 unaffected sisters. Proband also diagnosed with triscaphe and thumb DIP OA. Had total knee and hip arthroplasty. Daughter also diagnosed with spine OA.
SA735*	Glenohumeral OA - 3 affected. Proband (F), sister, and daughter. Sister has also had surgery for thumb CMC OA and has had bilateral total knee and hip arthroplasty.

* - Pedigrees in Supplemental Figure 1

A
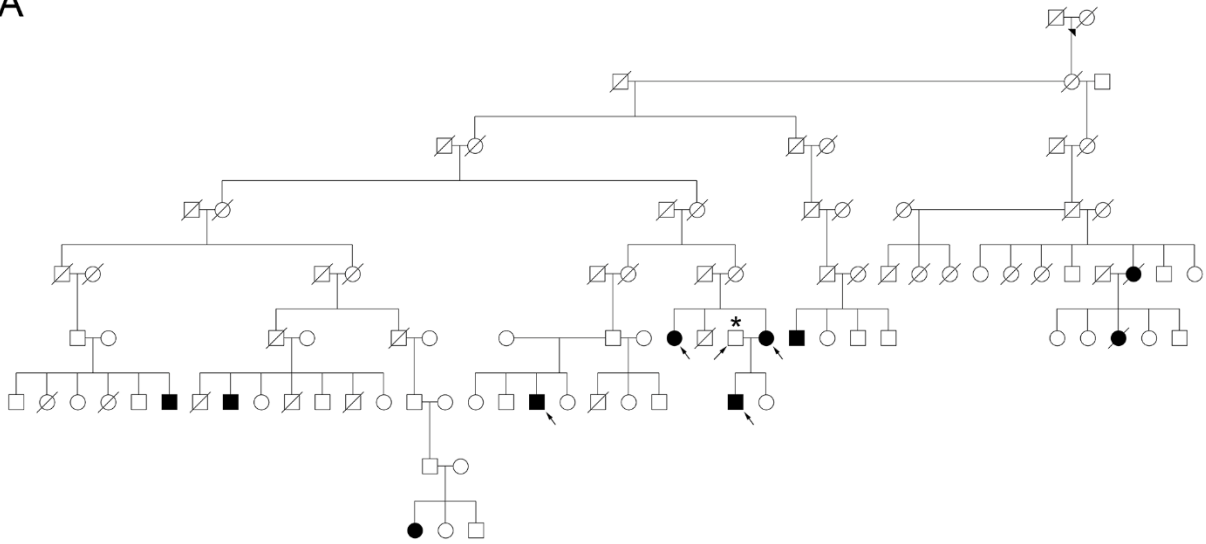
B
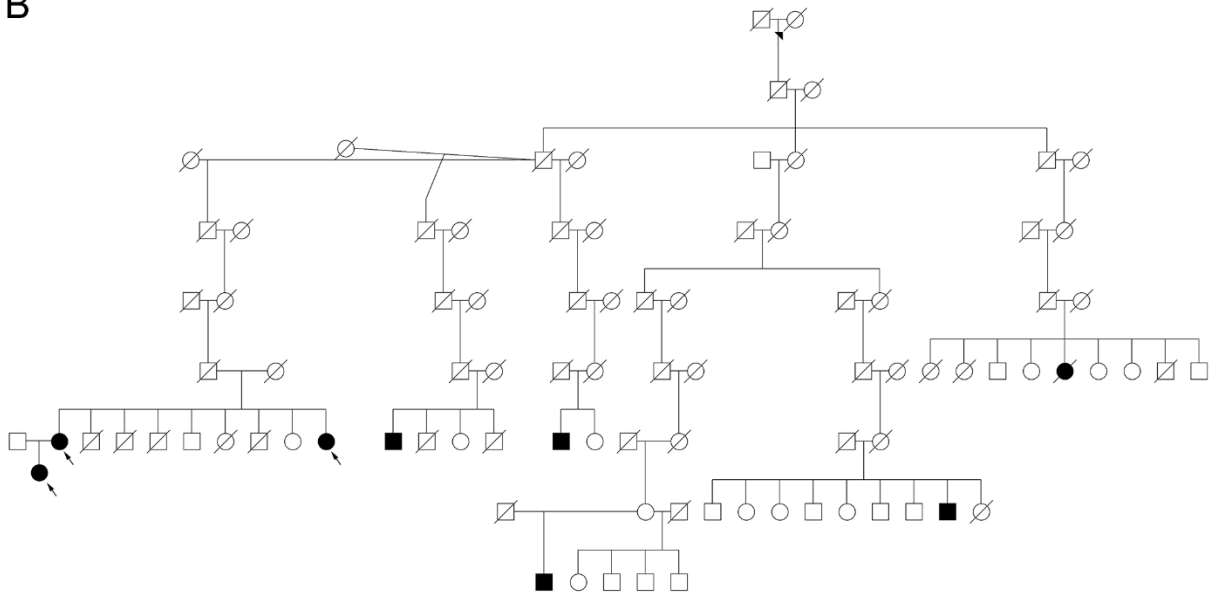
Supplemental Figure 1. Examples of high-risk osteoarthritis pedigrees. Two

multigeneration high-risk pedigrees segregating a, finger interphalangeal joint OA

(FIJ744 family, *NOD1*) and b, glenohumeral OA (SA7355 family, *IKBKB*) identified from

the Utah Population Database. The OA phenotype segregates as an apparent

autosomal dominant trait. Circles = females, squares = males, slash = deceased. Filled

circles/squares = affected individuals; open circles/squares = individuals with unknown
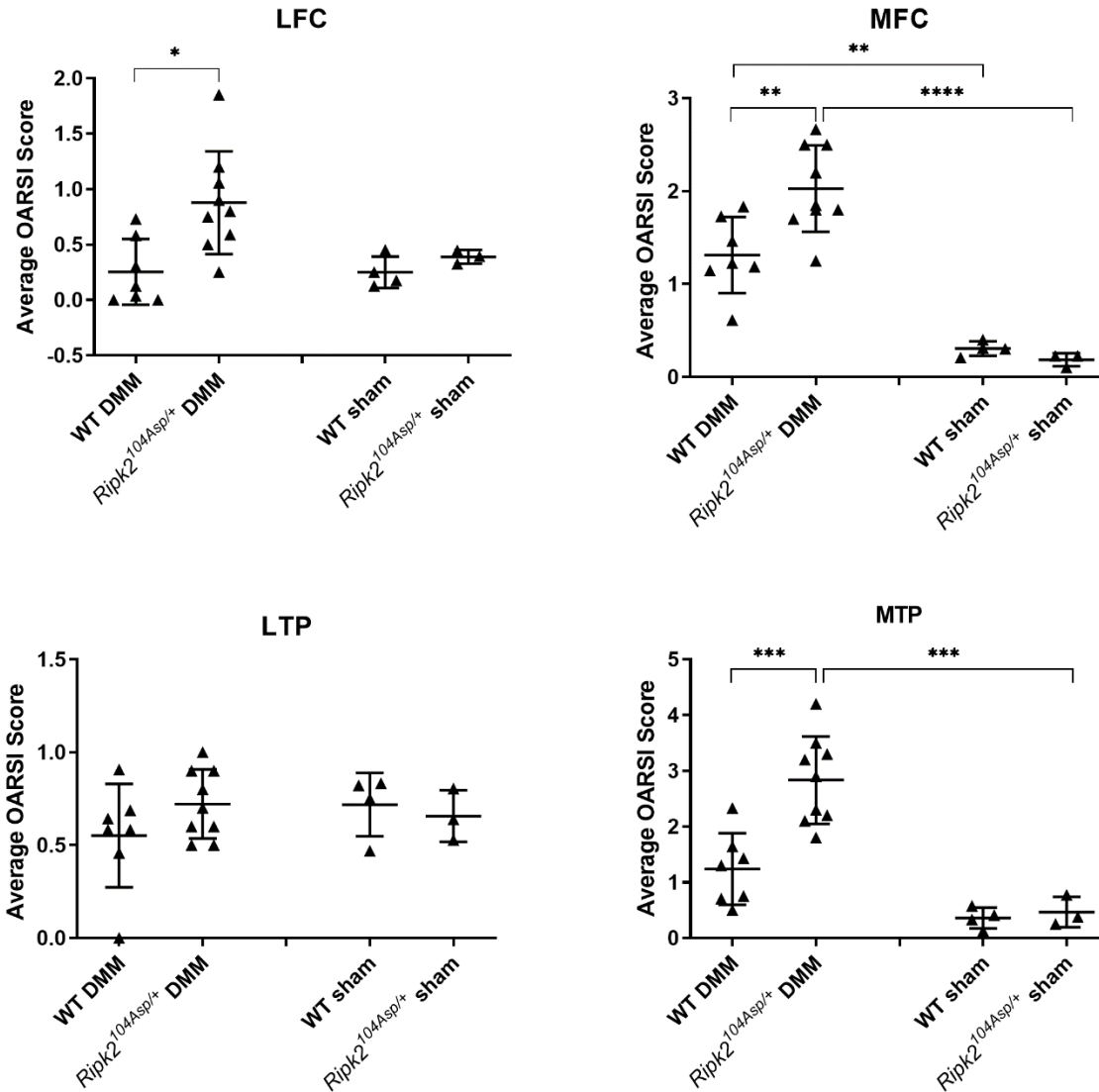
affection status. Arrowhead indicates the founder of each family. Arrows indicate individuals who were sequenced and used for genomic analyses. Asterisk in a indicates an unaffected individual who was sequenced and used for genomic analyses.
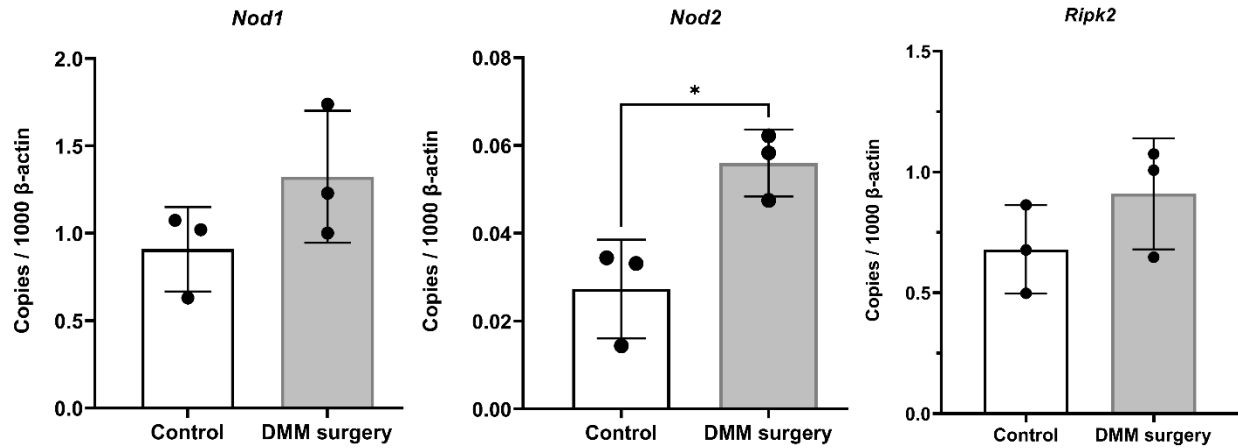
Supplemental Figure 2. *Nod1*, *Nod2*, and *Ripk2* are expressed in the uninjured joint and the pathway is activated in response to joint injury. qPCR analysis of *Nod1*, *Nod2*, and *Rlpk2* expression using RNA isolated from whole joints 10 days after DMM surgery. Error bars represent ±SD and a statistically significant difference of P ≤ 0.05 (*) was determined by a two-tailed unpaired t-test.
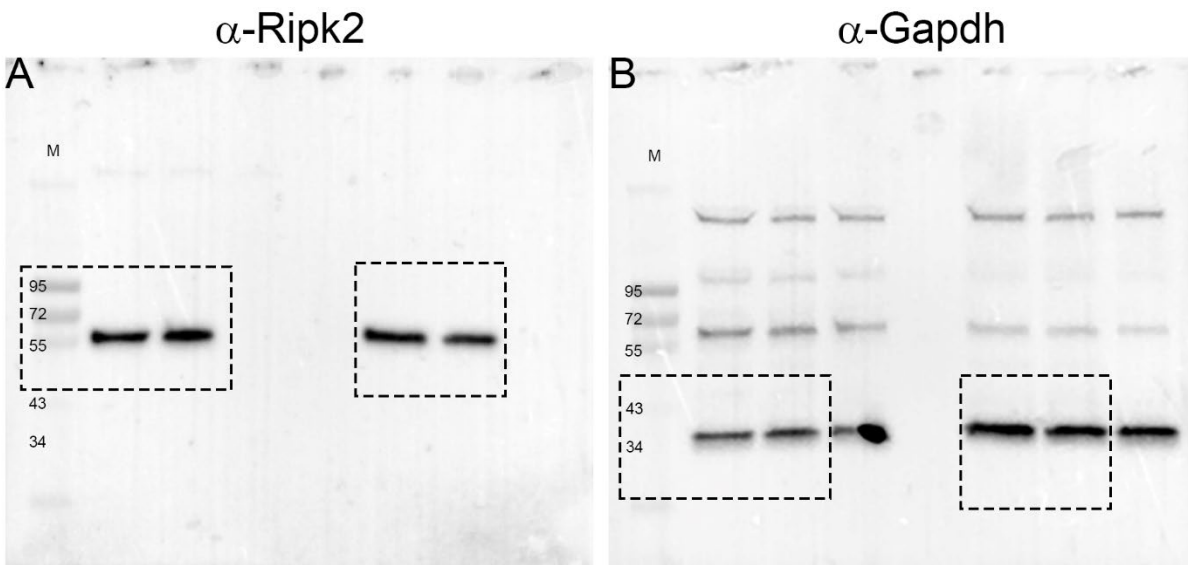
Supplemental Figure 3. Unmodified Ripk2 and Gapdh immunoblots used to generate data in figure 1B. (A) The D10B11 antibody (Cell Signaling Technology) was used to detect Ripk2. (B) the sc-365062 antibody (Santa Cruz Biotechnology) was used to detect Gapdh. Dashed boxes indicate the portion of immunoblots that were used in figure 1B. M = protein mass standards in kDa.

Supplemental Figure 4. WT and *Ripk2*[104Asp] primary chondrocytes respond to NOD2-stimulation by MDP. (A) WT and B) *Ripk2*[104Asp] primary chondrocytes were treated for 6 hours with 10 µg/mL MDP to activate the NOD2/RIPK2 pathway. (A) Volcano plot illustrating genes significantly upregulated (red) or downregulated (blue) following stimulation of WT primary chondrocytes with MDP. (B) Volcano plot illustrating genes significantly upregulated (red) or downregulated (blue) following stimulation of *Ripk2*[104Asp] primary chondrocytes with MDP. The nCounter Fibrosis panel was used for all experiments.

Supplemental Figure 5. Regional analysis of the severity of OA in WT and *Ripk2*[104Asp] joints subjected to sham or DMM surgery. Quantification of average OARSI scores of joints in 8-week post DMM WT sham (n=3), *Ripk2*[104Asp] sham (n=4) , WT DMM (n=7), and *Ripk2*[104Asp] DMM (n=9) mice. LFC = lateral femoral condyle, MFC = medial femoral condyle, LTP = lateral tibial plateau, MTP = medial tibial plateau. Error bars represent ±SD and statistically significant differences of P ≤ 0.05 (*), P ≤ 0.01 (**), P ≤ 0.001 (***), and P ≤ 0.0001 (****) were determined by two-way ANOVA with Tukey's multiple comparisons test.
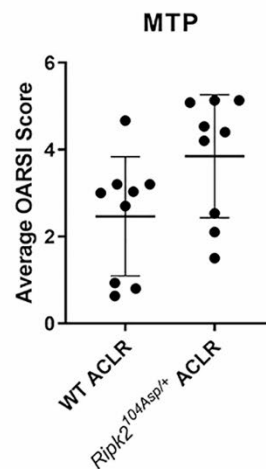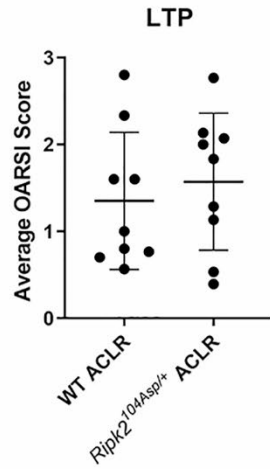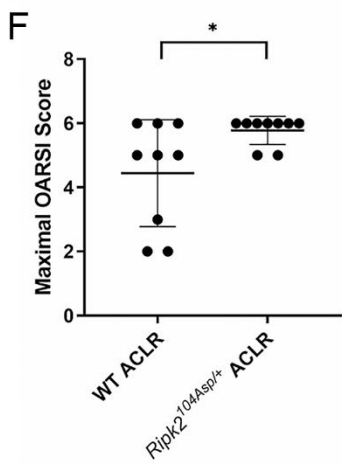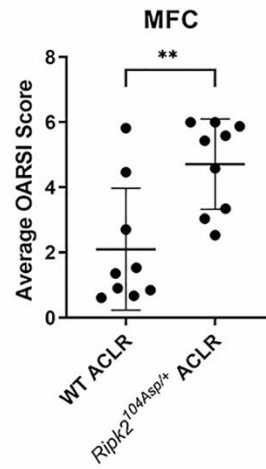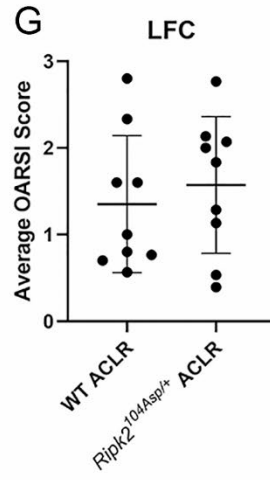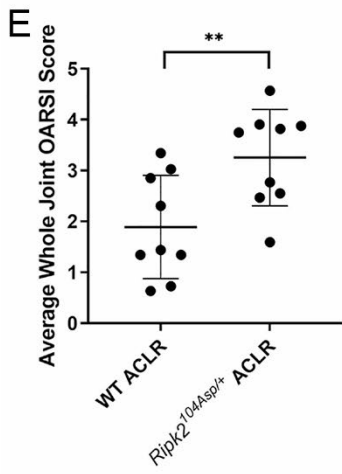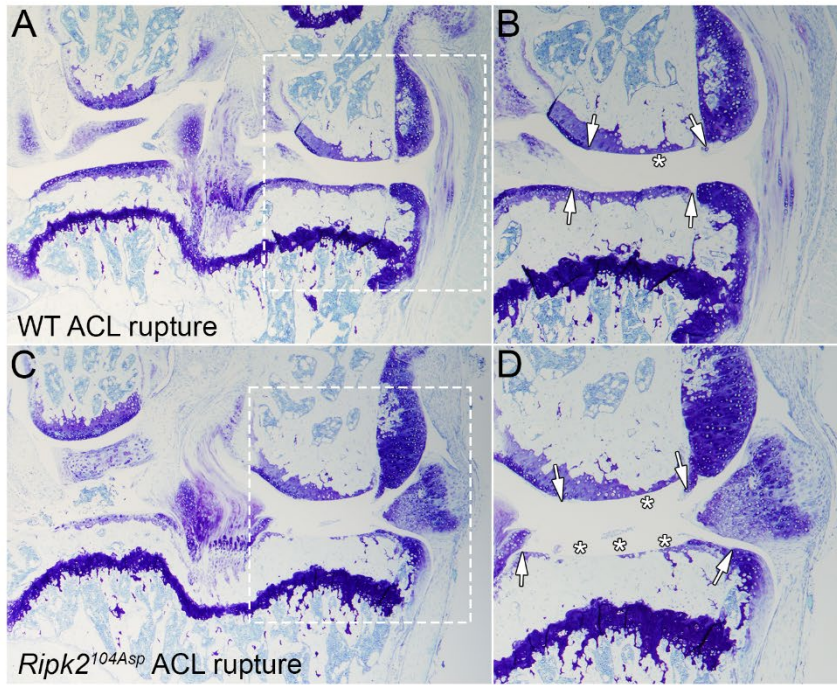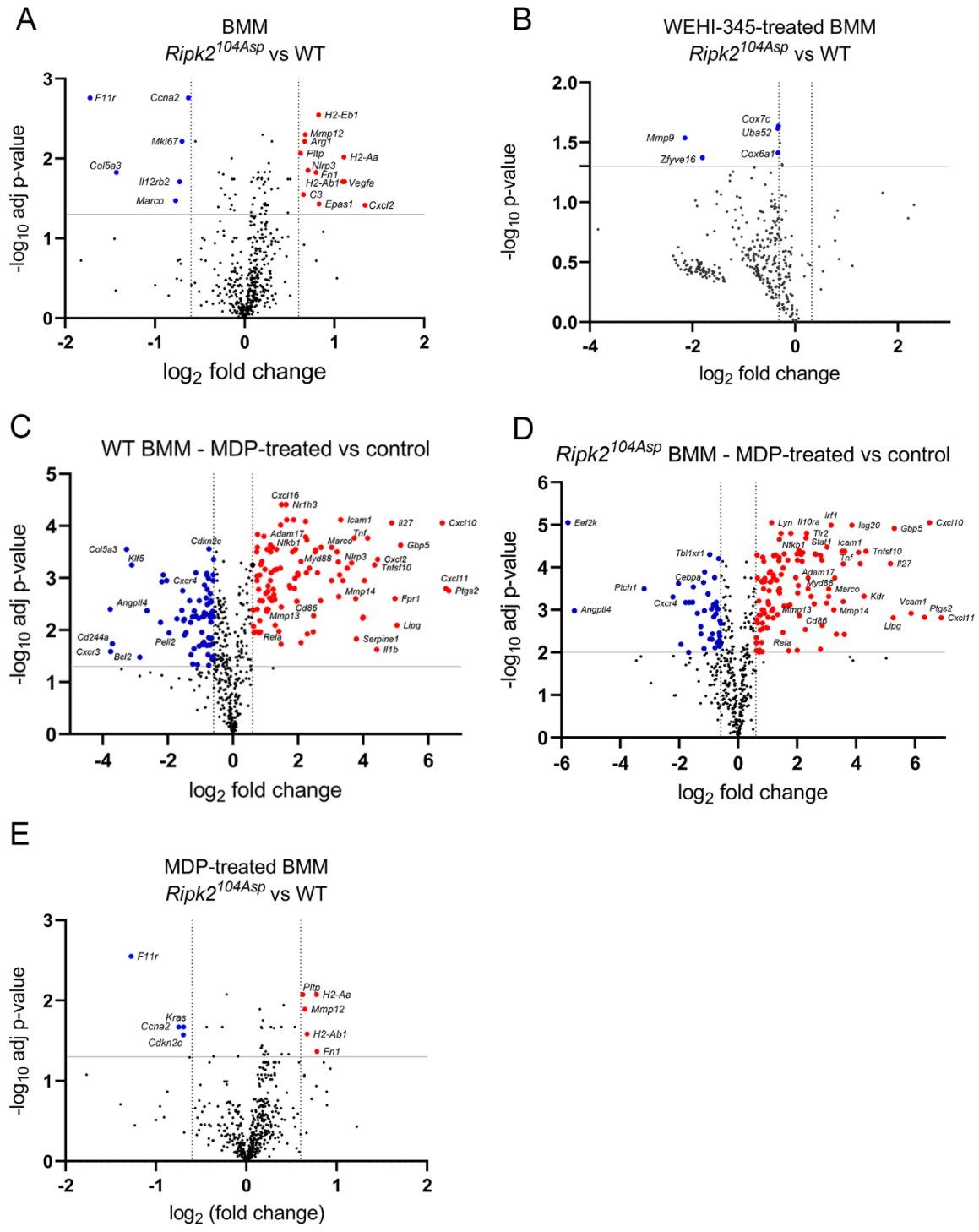
Supplemental Figure 6. The *Ripk2^{104Asp}* allele acts dominantly and is sufficient to confer increased susceptibility to post-traumatic osteoarthritis induced by non-invasive ACL rupture. (A-D) WT and *Ripk2^{104Asp}* mice underwent non-invasive ACL rupture (ACLR) at 16-weeks of age and were analyzed at 5 weeks post-rupture. (A, B) Knee joints of WT mice subjected to ACL rupture displayed moderate/severe loss of proteoglycan content and cartilage (asterisk in B) on the medial side of the knee. The extent of damage is indicated by the arrows in B. (C, D) Knee joints of *Ripk2^{104Asp}* mice subjected to ACL rupture displayed severe loss of proteoglycan content (arrows in D) and loss of cartilage that progressed down to the subchondral bone in the medial tibial plateau (asterisk in D). (E, F) Knee joints of *Ripk2^{104Asp}* mice subjected to ACL rupture have an increased average whole joint and maximal OARSI scores compared to WT controls. (G) Regional analysis of the severity of OA in WT and *Ripk2^{104Asp}* joints subjected to ACL rupture. Tissue sections were stained with toluidine blue. A and C are images of the entire knee joint. Dashed boxes are presented at higher magnification in B and D to visualize the medial side of the joint. Femur is up and medial is to the right in all images. LFC = lateral femoral condyle, MFC = medial femoral condyle, LTP = lateral tibial plateau, MTP = medial tibial plateau. WT ACL rupture (n=9) and *Ripk2^{104Asp}* ACL rupture (n=9). Error bars represent ±SD and statistically significant differences of $P \leq 0.05$ (*) and $P \leq 0.01$ (**) were determined by a two-tailed unpaired t-test.
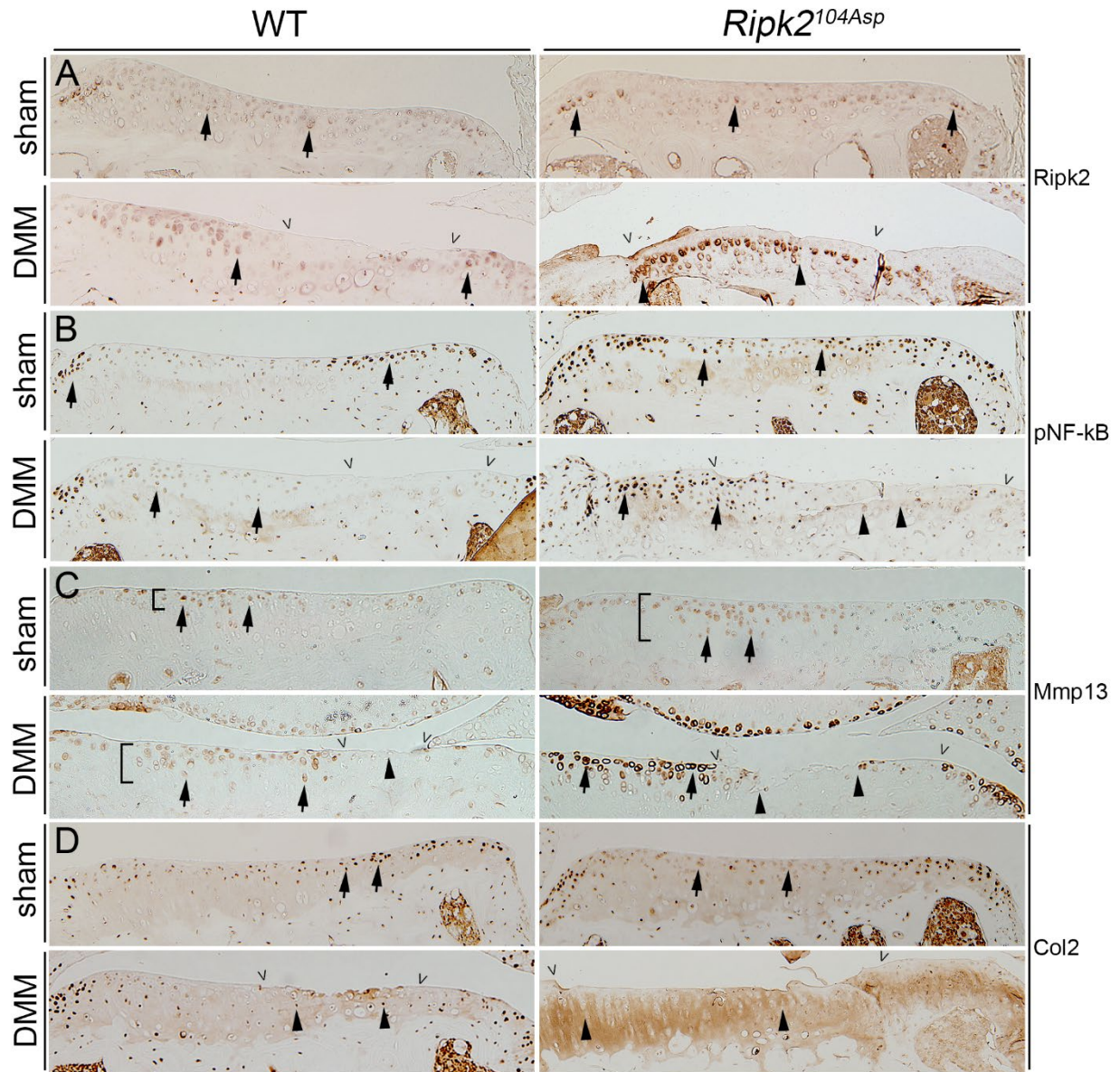
Supplemental Figure 7. *Ripk2^{104Asp}* enhances NOD/RIPK2 signaling as well as expression of OA-associated markers of matrix remodeling in uninjured joints and joints with PTOA. Immunohistochemical detection of (A) Ripk2, (B) pNF-κB, (C) Mmp13, or (D) Col2 in WT and *Ripk2^{104Asp}* mice 8 weeks following sham or DMM surgery. Images are of the medial tibial condyle. Selected regions from these images were used in figure

4. Arrows mark cells expressing Ripk2, pNF-κB, Mmp13, or Col2, arrowheads mark regions with severe cartilage damage, and V's mark the extent of cartilage damage.

Supplemental Figure 8. *Ripk2[104Asp]* acts dominantly and is sufficient to alter gene

expression in cultured BMM. Gene expression in BMM was measured using the

nCounter Fibrosis panel. (A) Volcano plot indicating genes with significantly altered expression in *Ripk2^{104Asp}* as compared WT cultured BMM. (B) Volcano plot indicating that very few genes are differentially expressed between *Ripk2^{104Asp}* and WT cultured BMM following treatment with the RIPK2 inhibitor, WEHI-345. (C) Volcano plot indicating genes with significantly altered expression following stimulation of WT BMM with MDP. (D) Volcano plot indicating genes with significantly altered expression following stimulation of *Ripk2^{104Asp}* BMM with MDP. (E) Volcano plot indicating genes with significantly altered expression comparing MDP-stimulated *Ripk2^{104Asp}* BMM with MDP-stimulated WT BMM.

REFERENCES

1.   Jurynec MJ, Sawitzke AD, Beals TC, Redd MJ, Stevens J, Otterud B, et al. A hyperactivating proinflammatory RIPK2 allele associated with early-onset osteoarthritis. Hum Mol Genet. 2018 Jul 1; 27(13):2406.

2.   Wang K, Li M, Hakonarson H. ANNOVAR: functional annotation of genetic variants from high-throughput sequencing data. Nucleic Acids Res. 2010 Sep; 38(16):e164.

3.   Hu H, Roach JC, Coon H, Guthery SL, Voelkerding KV, Margraf RL, et al. A unified test of linkage analysis and rare-variant association for analysis of pedigree sequence data. Nat Biotechnol. 2014 Jul; 32(7):663-669.

4.   Singleton MV, Guthery SL, Voelkerding KV, Chen K, Kennedy B, Margraf RL, et al. Phevor combines multiple biomedical ontologies for accurate identification of disease-causing alleles in single individuals and small nuclear families. Am J Hum Genet. 2014 Apr 03; 94(4):599-610.

5.   Wang H, Yang H, Shivalila CS, Dawlaty MM, Cheng AW, Zhang F, et al. One-step generation of mice carrying mutations in multiple genes by CRISPR/Cas-mediated genome engineering. Cell. 2013 May 09; 153(4):910-918.

6.   Wefers B, Bashir S, Rossius J, Wurst W, Kuhn R. Gene editing in mouse zygotes using the CRISPR/Cas9 system. Methods. 2017 May 15; 121-122:55-67.

7.   Glasson SS, Chambers MG, Van Den Berg WB, Little CB. The OARSI histopathology initiative - recommendations for histological assessments of osteoarthritis in the mouse. Osteoarthritis Cartilage. 2010 Oct; 18 Suppl 3:S17-23.

8.   Lewis JS, Hembree WC, Furman BD, Tippets L, Cattel D, Huebner JL, et al. Acute joint pathology and synovial inflammation is associated with increased intra-articular fracture severity in the mouse knee. Osteoarthritis Cartilage. 2011 Jul; 19(7):864-873.

9.   Christiansen BA, Guilak F, Lockwood KA, Olson SA, Pitsillides AA, Sandell LJ, et al. Non-invasive mouse models of post-traumatic osteoarthritis. Osteoarthritis Cartilage. 2015 Oct; 23(10):1627-1638.

10.   Jonason JH, Hoak D, O'Keefe RJ. Primary murine growth plate and articular chondrocyte isolation and cell culture. Methods Mol Biol. 2015; 1226:11-18.

11.   Marcu KB, Otero M, Olivotto E, Borzi RM, Goldring MB. NF-kappaB signaling: multiple angles to target OA. Curr Drug Targets. 2010 May; 11(5):599-613.

12.   Perkins JR, Dawes JM, McMahon SB, Bennett DL, Orengo C, Kohl M. ReadqPCR and NormqPCR: R packages for the reading, quality checking and normalisation of RT-qPCR quantification cycle (Cq) data. BMC Genomics. 2012 Jul 2; 13:296.

13.   Anders S, Pyl PT, Huber W. HTSeq--a Python framework to work with high-throughput sequencing data. Bioinformatics. 2015 Jan 15; 31(2):166-169.

14.   Maza E, Frasse P, Senin P, Bouzayen M, Zouine M. Comparison of normalization methods for differential gene expression analysis in RNA-Seq experiments: A matter of relative size of studied transcriptomes. Commun Integr Biol. 2013 Nov 1; 6(6):e25849.

15.   Love MI, Huber W, Anders S. Moderated estimation of fold change and dispersion for RNA-seq data with DESeq2. Genome Biol. 2014; 15(12):550.

16.   Morrison TB, Weis JJ, Wittwer CT. Quantification of low-copy transcripts by continuous SYBR Green I monitoring during amplification. Biotechniques. 1998 Jun; 24(6):954-958, 960, 962.